Research Article ISSN 2998-4513

International Journal of Cardiology and Cardiovascular Disorder

# High-Density Lasermapping Guided Catheter Ablation - Development and Application

**H Weber[1]*, L Schmitz[2], A Heinze[3], L Ruprecht[4] and M Sagerer-Gerhardt[1]**

[1]*CCEP Center, Section Research and Development, Taufkirchen, Taufkirchen, D-82024, Germany.*

[2]*Charité Berlin - Department of Pediatric Cardiology, Berlin, D-13353, Germany.*

[3]*Lasers and Applied Technologies Laboratory, Hospital Harlaching, Teaching Hospital of the Ludwig- Maximillian-University of Munich, Munich, D-81545 Germany.*

[4]*Laboratory Animal Facilities, Helmholtz Center Munich, Neuherberg, D-85764, Germany.*

***Corresponding Author**

**Helmut Weber,**
CCEP Center, Section Research and Development, Taufkirchen, Taufkirchen, D-82024,
Germany.

**Submitted**: 16 Dec 2025; **Accepted:** 22 Dec 2025; **Published** : 15 Jan 2026

**Citation:** Weber, H. et al., (2026). High-Density Lasermapping Guided Catheter Ablation - Development and Application.. *I J cardio & card diso; 7*(1):1-14. DOI : https://doi.org/10.47485/2998-4513.1052

**Abstract**

*High Density (HD) endocardial catheter mapping is used for precise localization and selective ablation of arrhythmogenic substrates in the heart. By using the myocyte specific 1064nm laser wavelength HD lasermapping allowed for monitoring of lesion formation in the myocardial wall during laser application. With timely stop of HD lasermapping guided ablation the lesion is limited to the myocardial wall sparing adjacent healthy myocardium and mediastinal structures including the esophagus, lungs, vagus etc. from thermal injury. HD lasermapping guided ablation is performed under normothermic conditions. It is a low power - short duration procedure. With its unique safety and efficacy characteristics it is more than just a viable alternative to traditional ablation techniques for ablation of cardiac tachyarrhythmias. With its large potential for further development e.g., artificial intelligence, and with its request for design to cost (DTC) for competitive products, HD lasermapping is unique and has a high potential for becoming an all pervasive catheter ablation procedure.*

**Keywords:** Catheter mapping; Catheter ablation; High-Density Lasermapping; Laser; Tachyarrhythmias.

## Introduction

Catheter ablation is a minimally invasive treatment used for various cardiovascular disorders (Weber et al., 2025). Catheter mapping is the prerequisite for catheter ablation of cardiac arrhythmias, for identification and localization of arrhythmogenic substrates in the heart. In general, mapping is performed by using multielectrode catheters manipulated under fluoroscopy to target and ablate arrhythmogenic substrates. Various systems for mapping and ablation of tachycardia are routinely used (Kim et al., 2020). We describe the development of the "high-density" (HD) laser catheter mapping and ablation technique, by using the 1064nm laser CardioVascLas® and the open-irrigated electrode laser mapping and ablation catheter RytmoLas® LasCor® GmbH.

## Methods and Results

### HD Catheter mapping

Supported by the DFG Project SFB89 Cardiology Göttingen, 1975 we have started with systematic electrode catheter exploration of the heart chambers in pediatric patients with cardiac arrhythmias in the department of pediatric cardiology of the Georg-August-University of Göttingen. By using bipolar 4F to 6F ring electrode catheters with narrow ≤2mm interelectrode distances (USCI catheter Instruments) electrical potentials suggesting specific potentials of accessory pathway (AP) were recorded during supraventricular tachycardia (SVT). Towards the end of the spontaneous SVT the AP potential amplitudes dwindled gradually. Simultaneously with the AP minimization (Fig 1) or disappearance (Fig 2) the SVT ended.

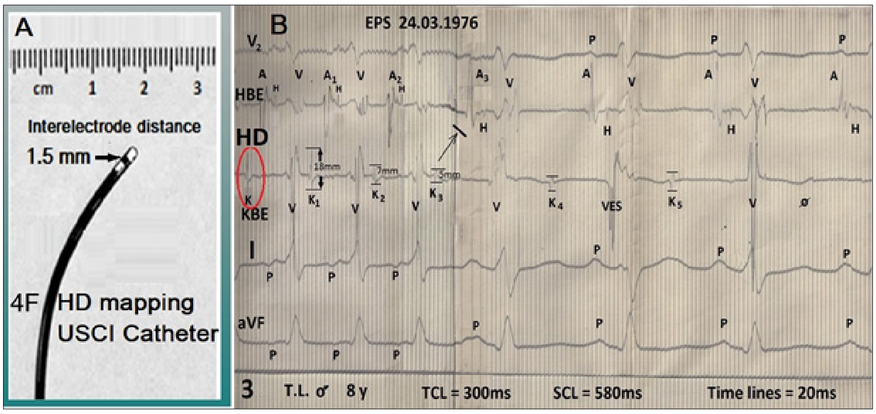


**Figure 1:** (A) Ring electrode catheter used for high density mapping. (B) Accessory pathway potential K (oval) gradually dwindled (K–K3). Simultaneously with the block of retrograde atrial activation (K3-A3 oblique arrow) the tachycardia ended. V, I, aVF = surface lead ECGs, HBE = His-bundle, HD KBE = High Density AP electrograms, A = atrial, V = ventricular potentials, P = P-wave, SCL = sinus cycle length, TCL = tachycardia cycle length.

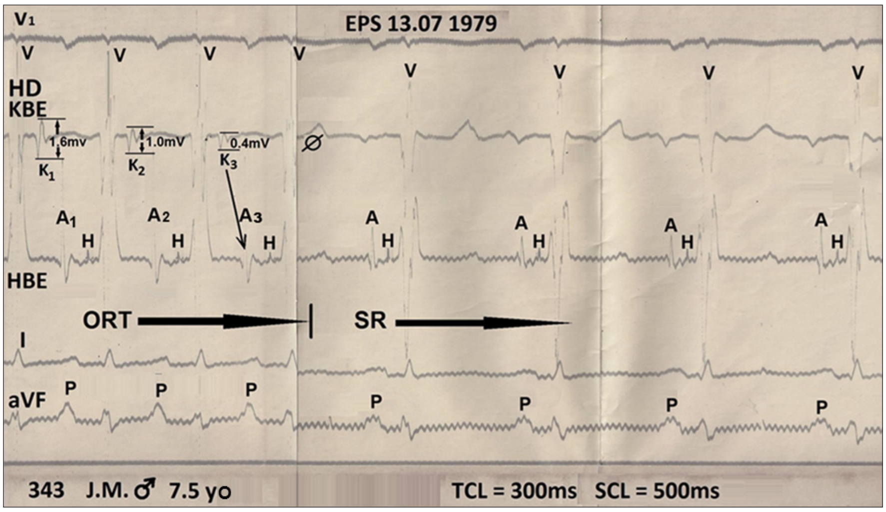


**Figure 2:** During spontaneous SVT the AP potential K is dwindling gradually and with the stop of retrograde atrial activation K3-A3 (arrow) K potential is abolished(Ø) the tachycardia is stopped simultaneously and sinus rhythm resumed

V, I, aVF = surface lead ECGs, HD KBE = High Density accessory pathway and HBE = His-bundle electrograms, ORT = orthodromic reentry tachycardia, SR sinus rhythm, A atrial, V ventricular potentials, EPS electrophysiological study, TCL tachycardia, and SCL sinus cycle length

Meticulous catheter exploration of the AV rings was required to localize the AP during the SVT in pediatric patients (Fig 3).

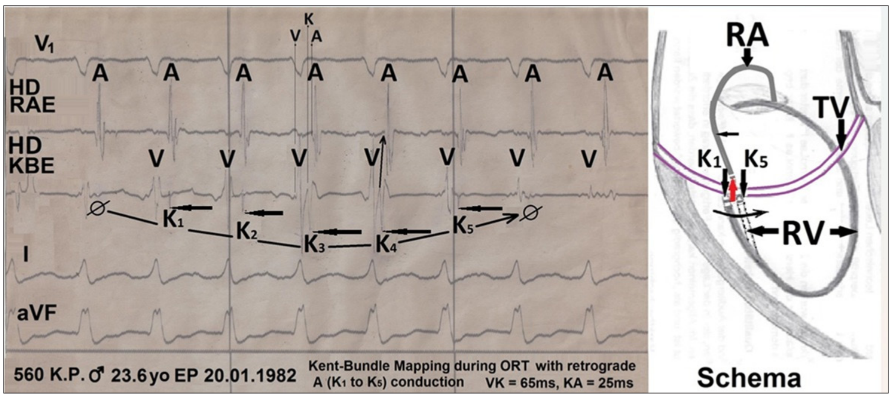


**Figure 3:** By mouving the catheter during SVT over the narrow gap of the tricuspid valve ring where the accessory pathway (K) is bridging the ring the AP potential K1 appears, its amplitude increase: K2-K3, decrease: K4-K5 and disappears (Ø).

V, I, aVF surface lead ECGs, HD RAE = high density right atrial and KBE = accessory pathway electrograms, A atrial, V ventricular, K accessory pathway potential. EP electrophysiological study. Schema: RA = right atria, RV = right ventricle and TV = tricuspid valve ring, and K1 K5 Catheter positions

Specific AP potentials were recorded also during sinus rhythm simultaneously with the Delta wave in the surface lead electrograms (Fig 4A).

In 1979 permanent atrioventricular block was induced inadvertently by DC cardioversion delivered to the His-bundle (Vedel et al., 1979). With our experience in high resolution mapping of specific AP potentials we intended to apply DC shocks for selective ablation of the AP with the aim to cure the patient from the SVT without inducing complete heart block with the subsequent need for permanent cardiac pacing. We have therefore tested DC-shock application in an experimental model (Weber et al., 1986) and in August 1982 a catheter mapping guided DC shock was aimed at an antero-septal AP in a patient with frequent SVT attacks and syncope (Weber & Schmitz, 1983). After the shock the AP potential was abolished and simultaneously the delta wave disappeared (Fig 4B).

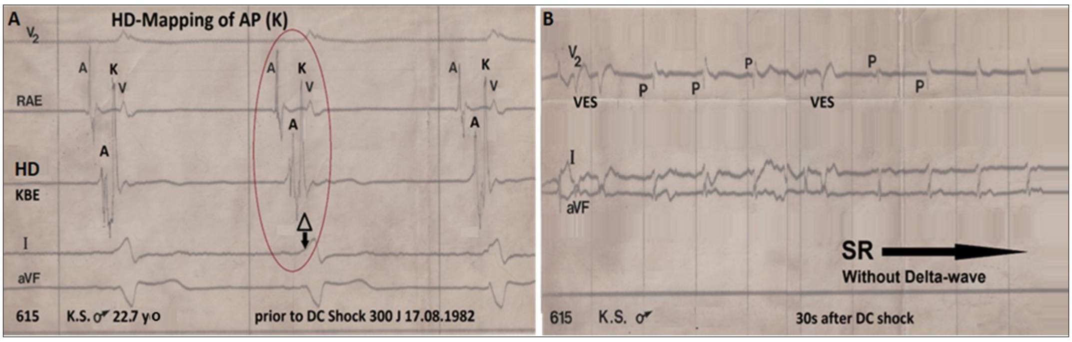


**Figure 4** : (A) Specific anteroseptal accessory pathway potential (K) recorded in the High Density (HD) mapping electrogram during sinus rhythm simultaneously with the delta wave (Δ) in the surface lead electrograms (oval)
(B) After DC-shock aimed at that area K potential and delta wave vanish simultaneouslyV, I, aVF surface lead ECGs, RAE = right atrial and HD KBE = high density accessory pathway electrograms, A = atrial, V = ventricular, and K = accessory pathway potentials. VES = ventricular Extrasystole, SR = Sinus rhythm Catheter technique for closed-chest ablation of an accessory atrioventricular pathway. H Weber, L Schmitz. New Engl J Med 308:653-654, 1983

The patient was cured permanently from its cardiac arrhythmia and remained asymptomatic (FUp >10y). This was our first High-Density (HD) cathetermapping guided ablation of an arrhythmogenic substrate in the heart. However, in the following years severe barotrauma caused by DC-shocks, high recurrence rate, even deaths were reported. After a 5 year follow-up of VT ablation in 51 patients recurrence occurred in 57%. Overall mortality with 16% was also high (Trappe et al., 1994). To overcome these limitations, we have used experimentally alternative power sources including the laser for HD catheter mapping guided ablation.

## HD Laser Catheter Mapping

Ought to its low absorption in water and intense scattering in turbid tissue, such as the myocardium, the 1064nm laser wavelength was found optimal for myocyte selective ablation (Boulnois, 1986). Initially, a Nd:YAG lasers 40N/4060N (MBB Dornier Ottobrunn, Germany) was used in in-vitro and in-vivo experiments. To improve handling and efficacy of the ablation procedures a diode laser with integrated irrigation pump and esophageal sensor was developed by LasCor® and was manufactured by Omicron Laserage Rodgau, Germany (Fig 5).

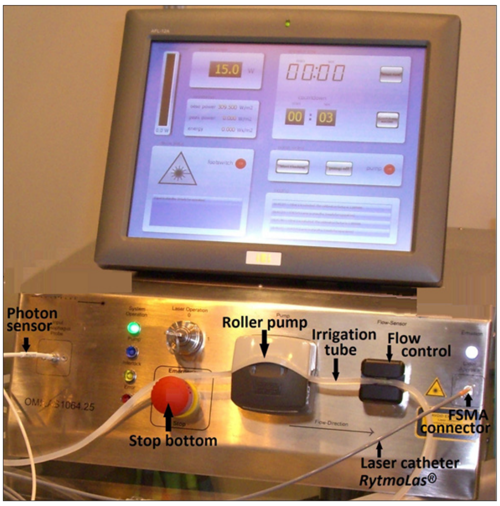


**Figure 5 Compact Diode laser CardioVascLas®**

Touch screen with power set at 15.0 Watt

- photon sensor for esophageal registration
- red emergency stop button
- integated roller pump for catheter irrigation
- tube for catheter irrigation
- ultrasound flow and particle control
- FSMA connector laser catheter RytmoLas®

To allow for HD laser catheter mapping as performed with the ring electrode catheters three 5mm pin-electrodes with interelectrode distances ≤ 2mm were mounted longitudinally on the laser catheter distal end (Fig 6). HD-mapping electrograms could be recorded in all three bipolar recordings only when the catheter was overriding precisely the His-bundle (Fig 6, C).

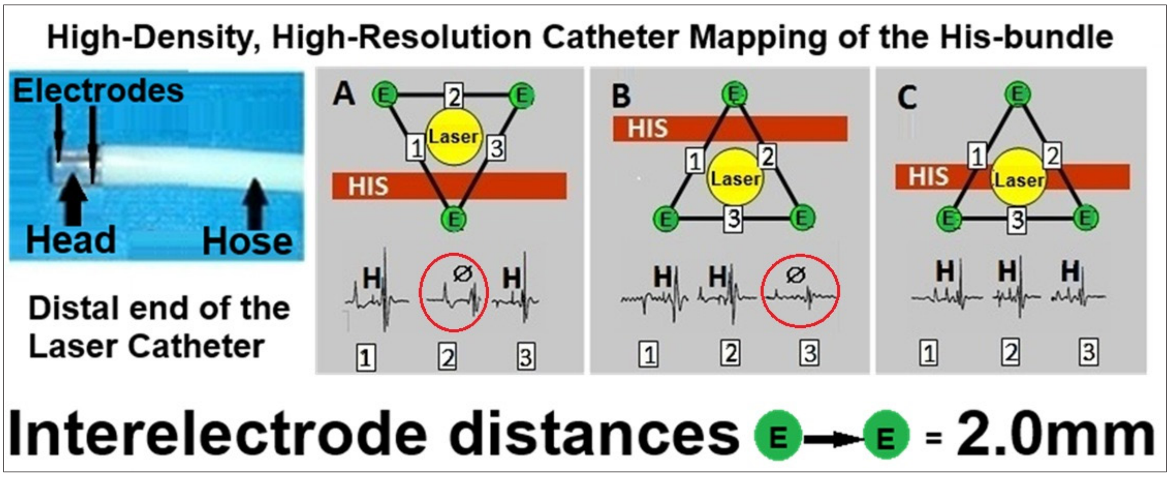


**Figure 6:** left Distal end of the laser catheter provided with cable electrodes. Schematically in A and B: slight lateral catheter positioning upon the His-bundle without H potential Ø (ovals). C: His Potential (H) in all recordings when framing the His-bundle with the electrodes symmetrically. This Figure demonstrates precise specific electrical potential recordings by HD laser catheter mapping

With this geometrical electrode configuration, a very precise localization of laser application limited to the targeted myocardial area was feasible. To achieve that, an optical fiber was mounted coaxially with its conically shaped tip 1.2 mm from the catheter endhole that allowed for a noncontact mode of laser application avoiding fiber to tissue direct contact, what would burn the tissue, destroy the catheter, and endanger patients. In addition, continuous saline catheter irrigation by means of the roller pump hindered blood penetration into the catheter lumen and, most importantly, created a clear pathway for the laser light to the myocardial area laser application was aimed at. HD laser catheter ablation was demonstrated during a workshop in the electrophysiology (EP) laboratory of the Duke University Medical Center North Carolina (Svenson RH, Littmann L, Splinter R) and in the EP laboratory of the UCLA supported by the LasCor® GmbH, Mr. Webster, and Dr. Helmy (Santa Monica, CA). 2010 and 2011 in-vivo experiments were performed at the Heart Rhythm Institute and Department of Medicine, University of Oklahoma, Oklahoma City, OK (Fig 7).

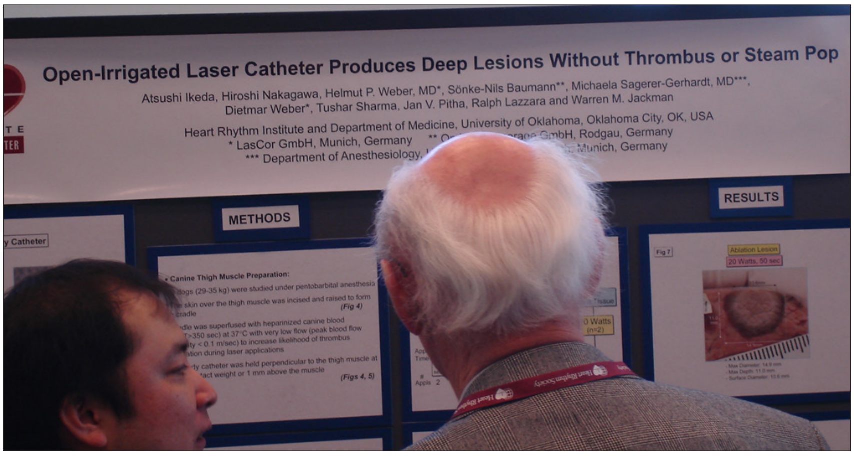


**Figure 7:** Poster presentations at the Heart Rhythm 32nd Annual Scientific Sessions May 4-7, 2011, San Francisco . CA, USA

The laser catheter produced deep clear-cut lesions without thrombus formation or steam pop (Atsushi et al., 2011). 1064nm laser application is performed under normothermic conditions. The catheter is not heated up; it does not transmit heat. Heat is induced deep intramurally by selective photon absorption by myocites and is spreading centrifugally in the myocardial wall. HD laser catheter mapping is practicable because electrical potentials can be recorded without electrical hum during laser application.

Laser aimed at the earliest electrical activation and highest potential amplitudes in the sinus nodal area induced gradual abatement of potential amplitudes and gradual lengthening of sinus cycle lengths (Weber et al., 2018). Thereby, amplitudes of local electrical potentials were reduced to those of the normal sinus nodal area but were not abolished. In the same time sinus cycle lengthened

(Fig 8A). More importantly, normal chronotropic competence was maintained. The lesion induced is a clear-cut homogeneous fibrous scar in the irradiated diseased area (Fig 8B).

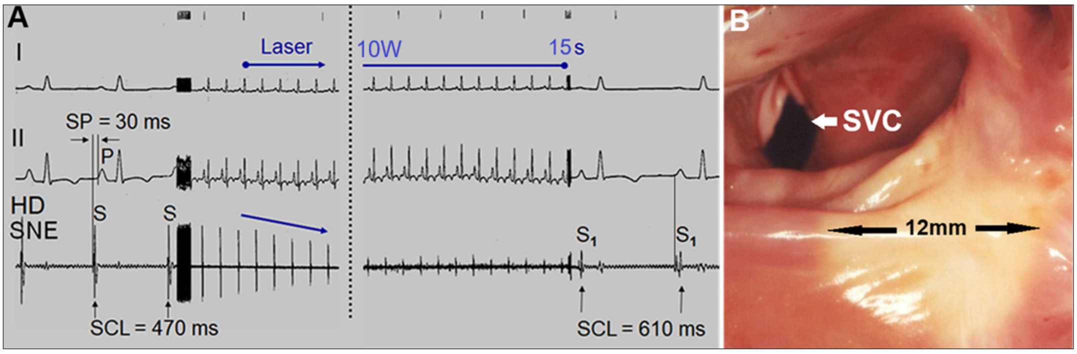


**Figure 8: (**A) Laser modulation of the sinus node. Gradual dwindling of sinus nodal electrical potential amplitudes (oblique arrow) and gradual lengthening of sinus cycle lengths (SCL 470 to 610ms). Earliest activation (SP-P = 30s) is abolished (vertical lines). (B) Endocardial view of the laser scar produced in the right atrial roofI, II surface lead electrograms, HD SNE = High Density Sinus Nodal Electrogram, SCL = Sinus Cycle Lenth, SP = Sino-Atrial conduction interval J Innovations CRM 9;3232-3238, 201

Laser aimed at the right atrial free wall induced gradual dwindling of electrical potential amplitudes until permanent abolishment was achieved (Fig 9 A). However, after timely stop of the laser prior to permanent abolishment of electrical potential amplitudes conduction shortly resumed and the height of amplitudes normalized (Fig 9 B).

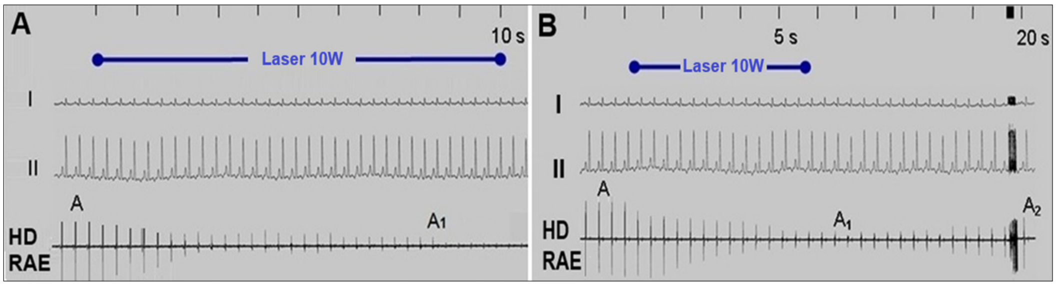


**Figure 9: (**A) Gradual dwindling and permanent abolishment of atrial potential amplitudes AA1. (B) Stop of laser application prior to permanent abolishment of atrial potential amplitudes AA1 with gradual recovery and normalization of amplitudes A1A2 I, II = surface lead electrograms, HD RAE = High-Density right atrial electrograms

Permanent abolishment of electrical potential amplitudes produced extensive clear-cut homogeneous transmural atrial scars without tissue vaporization with crater formation (Fig 10).

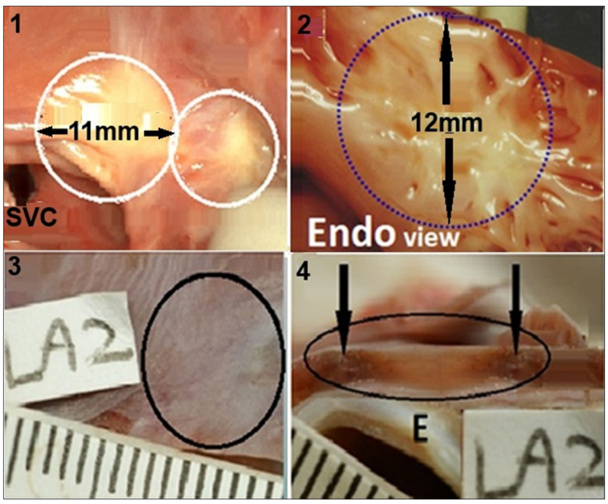


**Figure 10:** HD-Lasermapping guided clear cut homogenous transmural right (1,2) and left (3,4) atrial laser lesions at 10W without tissue vaporisation with crater formation SVC = superior Vena Cava, Endo = endocardial, E = esophageal wall.

Laser aimed at the atrial segment of the His-bundle induced gradual dwindling of atrial and His-bundle potential amplitudes and gradual lengthening of the atrio His, the proximal AV conduction time (Fig 11).

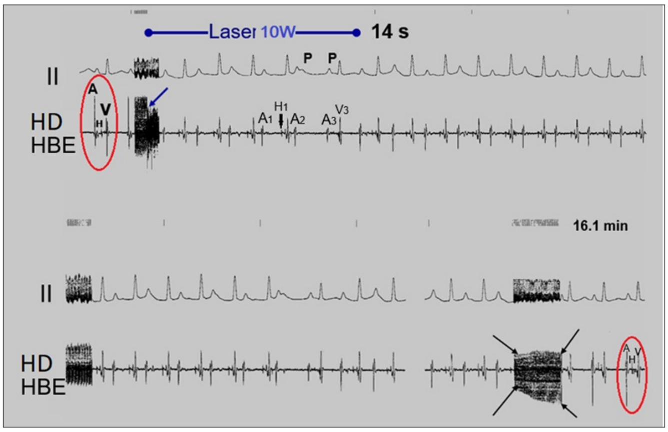


**Figure 11:** Gradual dwindling of atrial potential amplitudes AA1 and lengthening of the AH interval ($A_1H_1$) with the start of the laser (oblique arrow top). After stop of radiation with the first conduction block ($A_2$-$A_3$) atrial potential amplitudes and AH conduction gradually normalized (arrows and ovals).
II = surface lead electrogram, HD HBE = High-Density His-bundle electrogram, A atrial, H His-bundle, V ventricular potentials

Laser application aimed at penetrating bundle blocked atrio-ventricular conduction but after timely stop of radiation conduction shortly resumed (Fig 12).

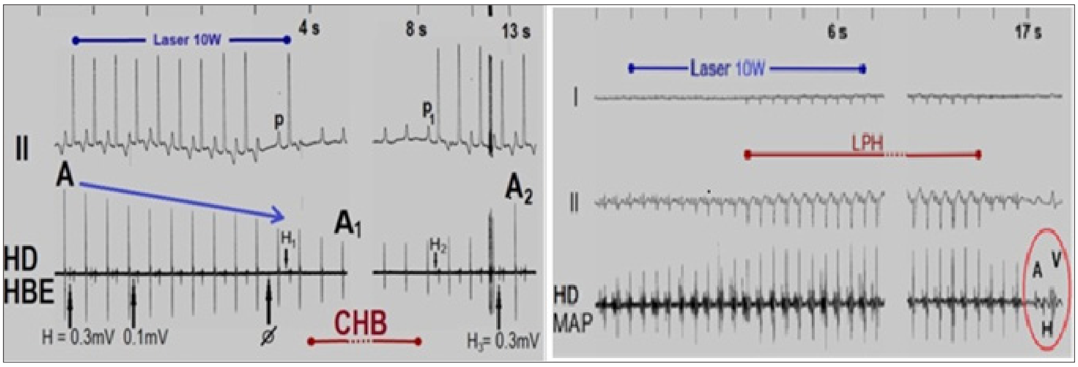


**Figure 12:** (A) Gradual dwindling of atrial AA1 and His potential HH1 amplitudes during laser application (oblique arrow). Timly laser stop after the first His-bundle block Ø allowed for complete recovery of both atrial (A1A2) and His-bundle potentials (H1H2) amplitudes. II = surface lead electrogram, HD HABE = High-Density His-bundle electrogram, P = P-waves, A = atrial and H = His-bundle potentials, CHB = complete heart block (B) Left axis deviation during laser application aimed at the fascicular segment of the His-bundle and complete recovery of conduction in the 17th second (oval). I,II surface lead, HD HBE = High Density His bundle, HD LFE = High Density Left Fascicular Electrograms, P = P waves, A = atrial, H = His-bundle, V = ventricular potentials, LPH = Left Posterior Hemiblock.

However, after permanent block the His-bundle is replaced by fibrous tissue (Fig 13).

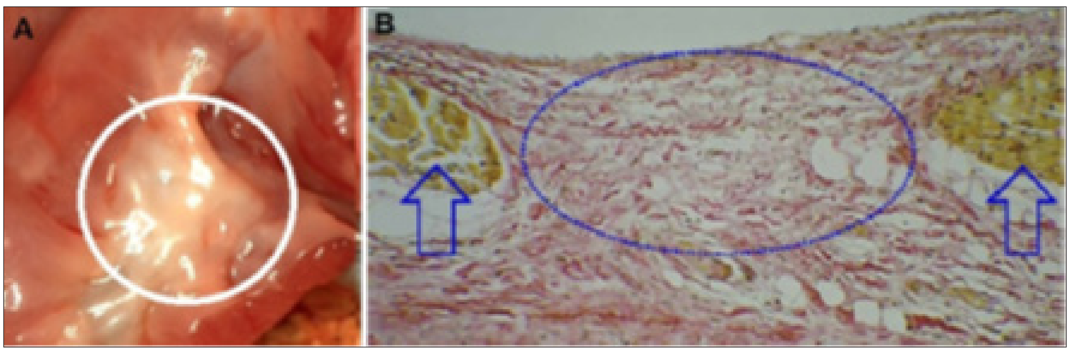


**Figure 13:** (A) Pale clear cut laser scar in the AV nodal area of a dog heart (Circle) (B) Fibrous scar interposed between the His-bundle stumps after laser induced complete heart block.

Radiation aimed at the left ventricular free wall induced gradual dwindling and permanent abolishment of local electrical potentials resulting in a transmural coagulation necrosis of the myocardial wall (Fig 14).

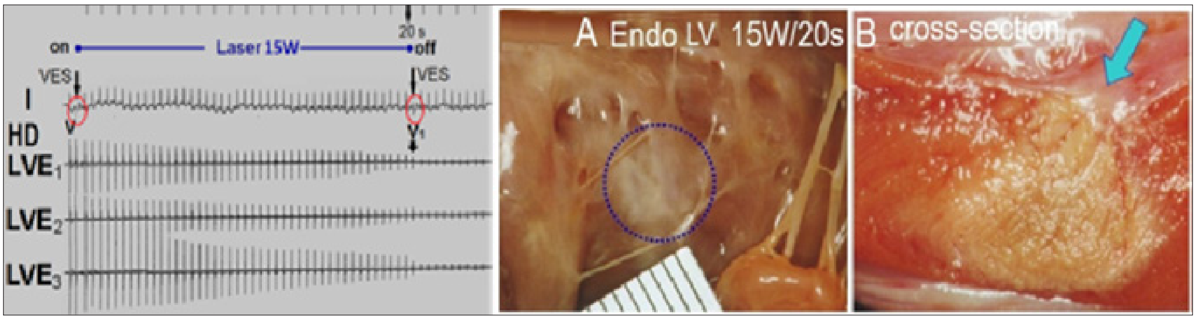


**Figure 14:** Gradual dwindling of electrical potential amplitudes (VV1) in the bipolar endocardial recordings during laser application aimed at the left ventricular free wall by using the catheter RytmoLas® Note: the ventricular extrasystole (ovals) induced by the start and stop of laser application (A) Transmural lesion thereby achieved in the left ventricular free wall in a dog model Endocardial view: coagulation necrosis shining through the normal transparent endocardium (Circle). (B) Transmural, homogenous, clear-cut lesion of coagulation necrosis. The arrow indicates the assumed catheter orientation during laser application

I surface lead, HD LVE = High density left ventricular electrograms, V = ventricular potentials.

Epicardial laser application aimed at the beating dog heart under video control displayed from the very beginning the myocardial coagulation process spreading radially. A transmural lesion without tissue vaporization with crater formation was achieved (Fig 15).


**Figure 15:** (A) Video start of epicardial laser application with a hand-hold catheter in vertical position upon the beating heart (arrow) (B )After 13s an intramural pale lesion of coagulation necrosis is shining through the undamaged Epicardium (circle) (C) The result is a transmural, clear-cut lesion without tissue vaporisation and crater formation.

Application of higher laser energy densities can produce thermal damages to adjacent mediastinal anatomic structures such as the esophagus, lungs, and nerves (Weber & Sagerer-Gerhard, 2014). Therefore, of crucial importance is to limit the time needed for ablation of arrhythmogenic structures. Excessive laser application increases the risk of thermal damage to adjacent healthy myocardium and neighboring anatomic structures including the esophagus, lungs, vagus nerve etc. Therefore, measurement of temperature was performed with an esophageal light sensor positioned behind the posterior left atrial wall. Under Xray control laser catheter applications were directed perpendicularly towards the esophageal sensor. A photon counter was adjusted for a laser stop when the maximum diode current was 60 µA or more and the maximum power measured was 150 µW or more, respectively. In-vitro and in-vivo laser applications were aimed at selected sides of the left atrial posterior wall (Weber et al., 2019).

Permanent abolishment of atrial potential amplitudes was achieved three to 5 seconds prior to the automatic stop of laser application by the esophageal temperature sensor (Fig 16).

**A** Table Time difference

| LA Lasing Time (s) | Permanent Abolishment of AP amplitudes (s) | Sensor Signal (s) | Time Difference (s) |
|---|---|---|---|
| 5 | AP recurrences | Ø | - |
| 10 | in 6 | 10 | +4 |
| 10 | 7 | 10 | +3 |
| 10 | 6 | 10 | +4 |
| 20 | 10 | 15 | +5 |
| 20 | 11 | 16 | +5 |
| 30 | 9 | 14 | +5 |
| 30 | 8s | 11 | +3 |
| 10W | Mean 8.14 s SD 1.95 | Mean 12.3 s SD 2.63 | Mean 4.14 s 3 - 5s |
| | $p$ = 0.0058 | | |

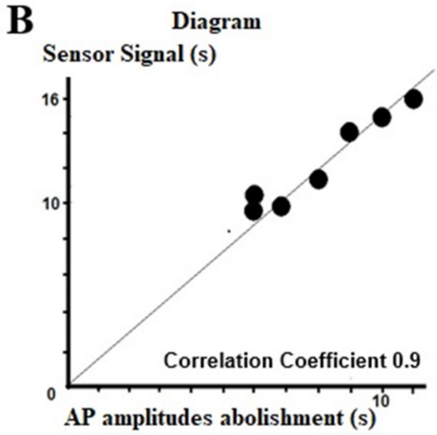


LA= left atrial, AP = atrial potential, s = seconds, SD = standard deviation, $p$ = $p$-value
By conventional criteria, this difference is considered to be very statistically significant.

**Figure 16:** (A) Time differences 3s to 5s between achievement of transmural myocardial lesion and the esophageal sensor signals 8 B) Diagram: Correlation Coefficient = 0.9.

With the automatic laser stop myocardial lesions were always transmural and importantly, limited to the myocardial wall, without thermal effects to adjacent healthy structures. A unique safety aspect of laser ablation.

## HD-Lasermapping

Unique HD-Lasermapping limits transmural lesion to the myocardial wall. Catheter orientation in perpendicular, oblique or flat positions may influence laser application time but it is not a major determinant for lesion formation. However, longer radiation times may be needed for transmural lesion formation (Sagerer-Gerhardt & Weber, 2016).The level of laser energy needed for transmural lesion formation may vary also with the thickness of the irradiated area of the myocardial wall. To assess depth of laser lesions various levels of energy were applied in an in-vivo thigh muscle model. Energy of 150J produced lesions at depth of up to 8.0 mm (Fig 17).

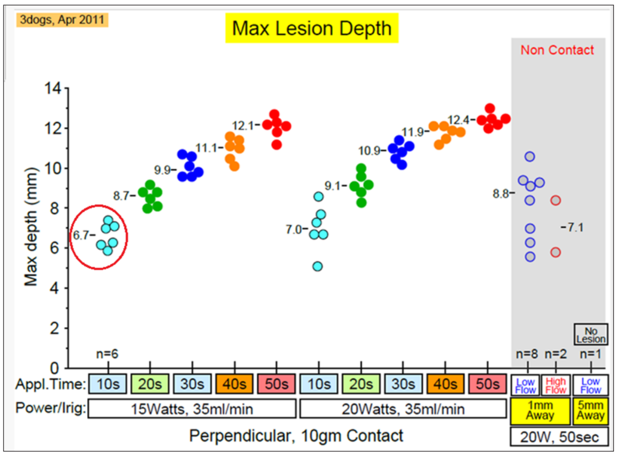


**Figure 17:** Lesion Depth achieved at various energy Levels: at 150J lesion Depth up to 8.0 mm is achieved (oval).

Maximum thickness of human atrial wall is ≤7.0 mm (Fig 18) and transmural atrial lesions can be achieved in ≤10s.

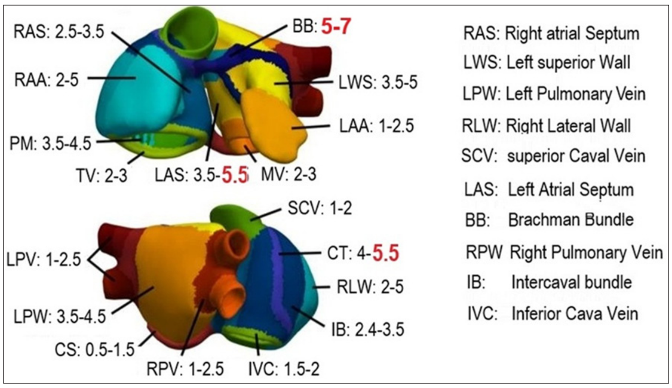


**Figure 18:** Atrial wall Thickness in mm at different regions.

Thus, energy settings for ablation of thin-walled atrial myocardium, e.g., for atrial fibrillation, were preset at 10W/10s and for ventricular myocardium at 15W/15s (Fig 21). The laser stops automatically after 10s or 15s respectively (Fig 19).

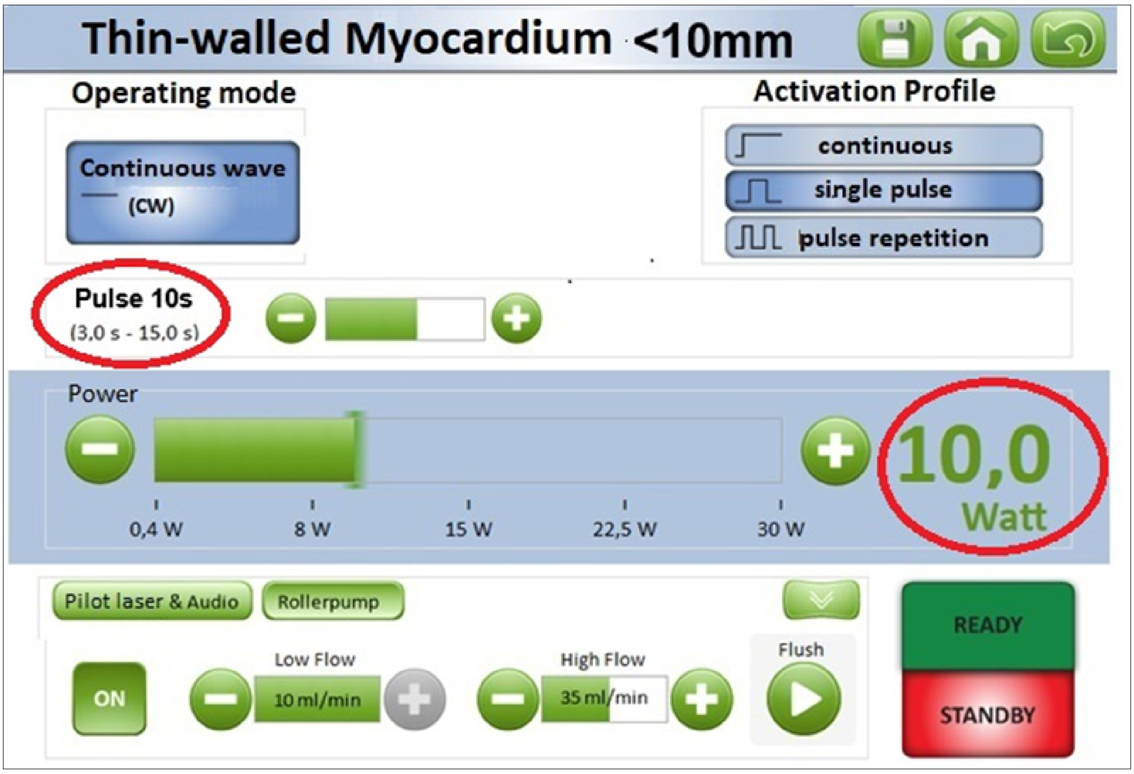


**Figure 19:** Preset energy setting for atrial and for ventricular arrhythmia ablation

If radiation is stopped automatically prior to permanent abolishment of potential amplitudes the lesion is not transmural, and the foot pedal must be pressed again until electrical potentials are abolished permanently. However, radiation should not be extended >5.0s because of possible deleterious effects such as pop, myo-cardial rupture, intramural bleeding or even perforation (Fig 20).

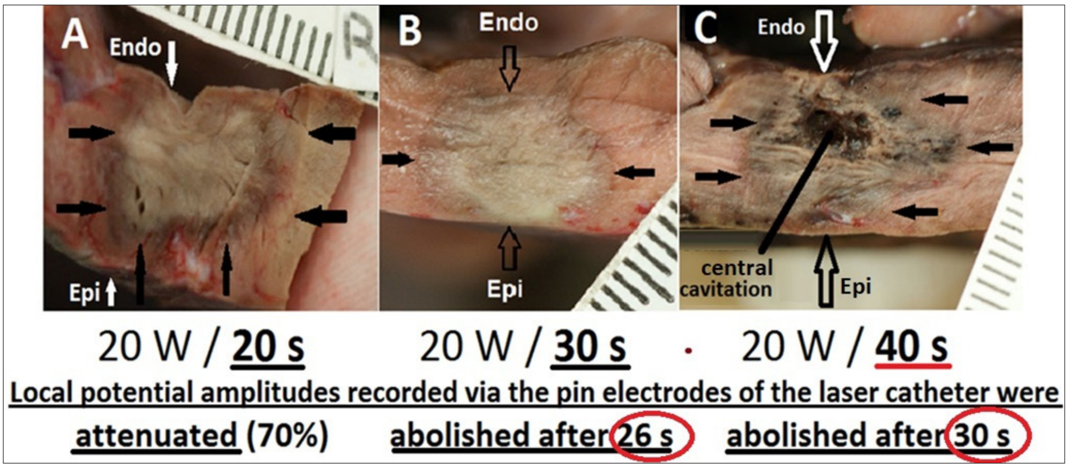


**Figure 20:** Ventricular lesions achieved with various energy settings: (A) prior to permanent abolishment of electrical potentials in the HD-Laser-mapping electrogram (B) 4s thereafter, when a transmural lesion is conspicuous (C) 10s thereafter with pop and intramural central cavitation (oblique Line).

Thickness of atrial walls may depend on types and location of arrhythmias, and comorbidities (Whitaker et al., 2016; Cunha et al., 2024; Słodowska et al., 2021). Ventricular walls may also vary widely especially in HOCM or hypertension (Nishimura et al., 2017; Obayashi et al., 2021).

The first attempt at HD-lasermapping guided ablation of an arrhythmogenic substrate was performed 1988-03-15th in a patient with an accessory left sided atrioventricular pathway with bidirectional conduction properties and with frequent syncope due to high rate ventricular activation causing episodes of ventricular tachycardia and fibrillation. The AP was connecting the ventricle over a very narrow gap in the lateral mitral ring close to the left descending coronary artery. Coronary angiogram performed prior to and after ablation showed a normal left coronary system without spasm or occlusion (Fig 21).

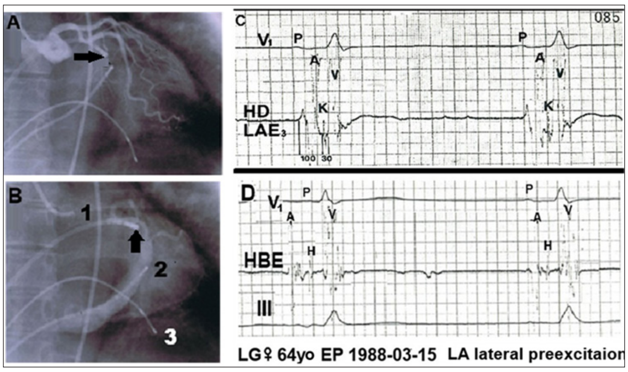


**Figure 21:** Normal coronary angiogram after laser ablation 10W/5s aimed at the left lateral accessory path-way during sinus rhythm (A) Angiogram of the left coronary (B) coronary sinus dye reflux (C) HD LAE3 = High Density laser catheter mapping of the accessory pathway potential K and (D) HBE = His-bundle elec-trogram with the His potential H
1 Angiogram catheter in the Aortic root 2 CS catheter 3 His catheter. The arrows indicate the tip of the laser catheter, V1, III = surface lead ECGs, A = atrial and V = ventricular potentials.

Laser catheter exploration of the left lateral mitral ring in the narrow segment where the AP bridged the mitral ring showed only in one of the three bipolar recordings specific accessory pathway potential during sinus rhythm and during orthodromic reentry tachycardia (Fig 22).

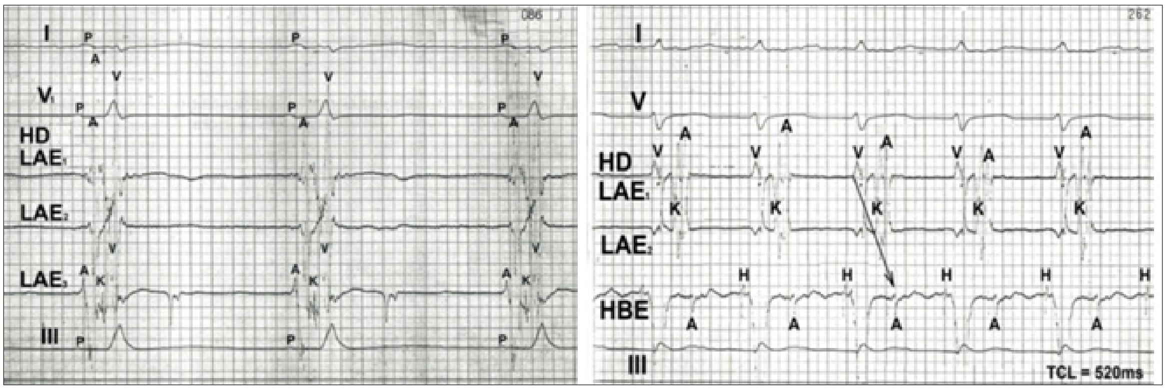


**Figure 22:** High Density left atrial electrogram (A) during sinus rhythm with the catheter in position as shown in figure 23. Only in HD LAE3 the specific accessory pathway potential K is displayed. (B) Bipolar High Density left atrial mapping electrograms during orthodromic reentry tachycardia with the catheter in position as shown in Figure 24. Activation sequence is from the left ventricle V over the specific accessory pathway K, to the earliest left atrial activation A in the HD LAEs and eventually to the A in the right atrial electrogram HBE (oblique arrow) I,V1,III = surface lead electrograms, HBE = His bundle electrogram, HD LAEs = High density left atrial elec-trograms, A = atrial; V = ventricular and K = accessory pathway (K) potentials, TCL = Tachycardia cycle length, p = P-waves.

During Multicenter study trials over 1000 HD-Lasermapping guided applications were performed in over 100 patients with various cardiac arrhythmias (Weber et al., 2017) including atrial fibrillation (Weber et al., 2017) without any kind of complications and with a success rate > 90%; long term follow up was 8.2 ± 6.5 years.

## Discussion

By using mapping electrode catheters with narrow ≤ 2mm interelectrode distances electrical potentials from a very small endocardial area were recorded. Thereby, as a random event, electrical potentials suggesting specific AP potentials were recorded for the first time 1975 during an SVT in the department of pediatric cardiology University of Göttingen (Fig 1,2,3,4). These were the first endocardial electrical potential recordings suggesting "High Density" catheter mapping. Only after 32 years, a new catheter with similar characteristics that enhances the assessment of lesion efficacy using electrogram amplitudes was described (Price et al., 2012). However, during Radiofrequency current or pulse field ablation the endocardial mapping electrogram is too short and is overlapped by electrical hum (Fig 23).

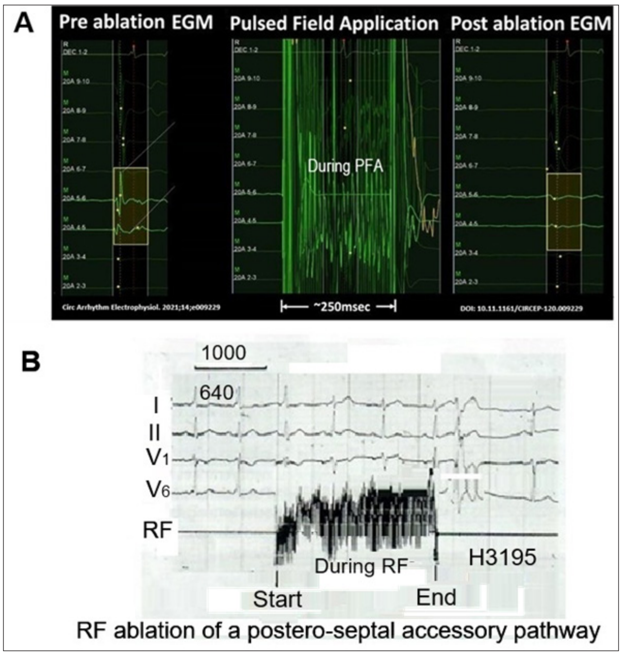


**Figure 23:** electrical hum during (A) pulse field (B) RF catheter ablation.

In contrast, during laser application gradual dwindling of electrical potential amplitudes within a few seconds is conspicuous on the monitor and with their abolishment the transmural lesion is limited to the myocardial wall (Fig 24).

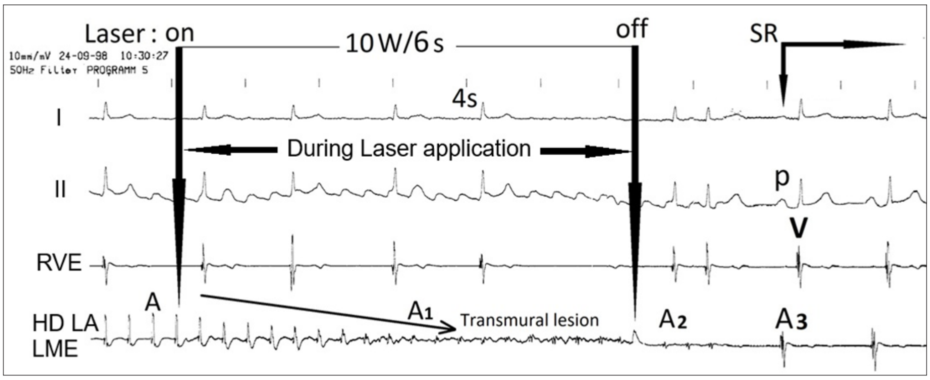


**Figure 24:** High Density Lasermapping guided ablation of long-lasting persistent atrial fibrillation. Gradual dwindling (oblique arrow) and abolishment of left atrial potential amplitudes after 4s of laser application aimed at the left atrial posterior wall. I, II surface lead electrograms, RVE = right ventricular electrogram, HD LA LME = High Density Lasermapping electrogram, A = atrial electrical potential, V = ventricular potential, p 0 P-wave, SR = Sinus Rhythm.

One of the specific advantages of HD-lasermapping is the ability to perform treatment under normo-thermic conditions. The catheter is not heated up, while avoiding interfering with the electrophysiologic monitoring principles. Immediate and real-time verification of the success of treatment on the monitor is extremely beneficial. The HD lasermapping, electrophysiologically guided ablation, allows for a systematic approach with simultaneous validation of initial success. Due to the homogenous tissue specific distributions of the 1064nm photon energy in myocardium the lesion results in a clear-cut solid volume of coagulation necrosis. As a result, when properly applied the laser lesion is transmural also when targeting thicker myocardial walls (Splinter, 2015). When other energy sources are used left atrial wall thickness correlates with pulmonary vein reconnection following atrial fibrillation ablation (Kushnir et al., 2025).

Laser lesions are not arrhythmogenic and render negligible risk of sustaining reentry pathways or reconnections in the treatment area. However, HD lasermapping at 15W/<30s on the posterior left atrial wall does not lead to visible damage to the esophagus but laser modulation of atrial ganglion plexi (GP) is thereby feasible and reduces inducibility of atrial fibrillation. No change in atrial effective refractory period is detected following ganglion plexi zones ablation when performed from the right atrium (Vakhrushev et al., 2024) but bi-atrial GP modulation can provide incremental benefits after both RA and LA ablation and starting ablation in the left atrium provides the most significant effect on vagal modulation (Francia et al., 2025). HD-lasermapping on GP modulation does not slow the heart rate and can consistently suppress AF long-term effect (Scherlag, 2015). In contrast, pulmonary vein isolation with the Farapulse TM PFA system is associated with only transitory and short-lasting effects on the autonomic nervous system which recover almost completely within a few minutes after ablation (Del Monte et al., 2024).

An important relatively new insight is that pulmonary vein isolation (PVI) is not enough for persistent AF ablation. Because vagal activation is a potent atrial AF trigger, whereas ventricular refractoriness remains unchanged facing extracardiac vagal stimulation (ECVS) and/or cardioneuroablation (CAN) underscoring chamber-specific autonomic effects and supporting the electrophysiological safety of ECVS and of CNA. ECVS and vagal AF induction test provide objective, reproducible functional end points to guide ablation strategy, confirm atrial vagal denervation, and potentially reduce AF recurrence. PVI plus GP ablation confers superior clinical results with less ablation-related left atrial flutter and reduced AF recurrence compared to PVI and linear lesion ablation at 3 years of follow-up (Fig 25).

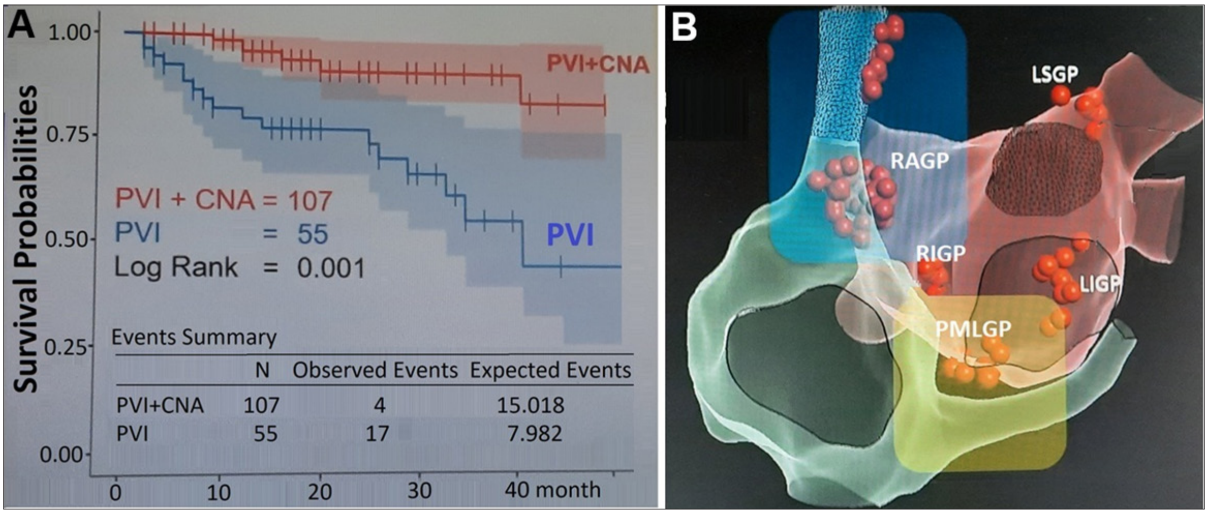


**Figure 25:** A Impact of Cardioneuroablation on Atrial B Location of retrocardiac ganglion plexi fibrillation ablation (PVI+CNA) LS=left superior, LI=left inferior, RA=right anterior.

Thus, cardioneuroablation substantially improves long term outcome of AF ablation (Pachon-M et al.,2025; Pokushalov et al., 2013). Lasermodulation of GP may have contributed to the high success rate of HD lasermapping of l-lpAF in our patients. During HD-Lasermapping guided ablation catheter manipulation is performed exclusively under Xray control and laser effects are visualized on the monitor. No other mapping system is used. In general, slight sedation and occasionally general anesthesia was applied in our multicenter study trials especially with respect to our pediatric patients.

HD-lasermapping guided ablation is unique. It represents disruptive technology in the field of cardiac electrophysiology and a paradigm shift in the treatment of cardiac arrhythmias. The accumulating body of evidence supports its unique safety and efficacy, positioning the laser as a key technology is more than just a viable alternative to traditional ablation techniques. The HD-lasermapping has a large potential for further development e.g., Artificial Intelligence (AI). Clinical integration of AI in AF management is a rapidly evolving field (Splinter, 2025). With the request for design to cost (DTC) for competitive products, the versatile unsophisticated HD lasermapping of the CardioVascLas® System is a highly competitive cardiovascular treatment option.

## Acknowledgement

Supported in part by LasCor GmbH. No conflict of interest.

## Conclusions

HD-Lasermapping is a minimally invasive, low power short duration procedure for the treatment of cardiovascular disorder, unique in safety and efficacy for tachyarrhythmia ablation.

## References

1. Weber, H., Heinze, A., Ruprecht, L., & Sagerer-Gerhardt, M. (2025). Minimally Invasive Laser Catheter Treatment of Cardiovascular Disorders. *I J cardio & card diso, 6*(4), 1-14. DOI: https://doi.org/10.47485/2998-4513.1050
2. Kim, Y. H., Chen, S. A., Ernst, S., Guzman, C. E., Han S., Kalarus, Z., Labadet, C., Lin, Y. J., Lo, L. W., Nogami, A., Saad, E. B., Sapp, J., Sticherling, C., Tilz, R., Tung, R., Kim, Y. G., & Stiles, M. K. (2020). 2019 APHRS expert consensus statement on three dimensional mapping systems for tachycardia developed in collaboration with HRS, EHRA, and LAHRS. *Journal of Arrhythmia, 36*(2), 215–270. DOI: https://doi.org/10.1002/joa3.12308
3. Vedel, J., Frank, R., Fontaine, G., & Grosgogeat, Y. (1979). Bloc auriculo-ventriculaire intra-Hisien définitive induit au cours d'une exploration endovasculaire droite. *Arch Mal Coeur Vaiss, 72*(1), 107–112. https://www.lissa.fr/rep/articles/107875
4. Weber, H., Schmitz, L., Dische, M. R., & Rahlf, G. (1986). Percutaneous intracardiac direct–current shocks in dogs: Arrhythmogenic potential and pathological changes. *Eur Heart J, 7*(6), 528-537. DOI:https://doi.org/10.1093/oxfordjournals.eurheartj.a062101

5. Weber, H., & Schmitz, L. (1983). Catheter technique for closed-chest ablation of an accessory atrioventricular pathway. *New Engl J Med, 308*(11), 653-654. https://pubmed.ncbi.nlm.nih.gov/6828100/
6. Trappe, H. J., Pfitzner, P., Fieguth, H. G., Wenzlaff, P., Kielblock, B., & Klein, H. (1994). Nonpharmacological therapy of ventricular tachyarrhythmias: observations in 554 patients. *Pacing Clin Electrophysiol, 17*(11), 2172–2177. DOI: https://doi.org/10.1111/j.1540-8159.1994.tb03821.x
7. Boulnois, J. L. (1986). Photophysical Processes in Recent Medical Laser Developments: a Review. *Lasers in Medical Science, 1*(1), 47-66. DOI: https://doi.org/10.1007/BF02030737
8. Atsushi, I., Nakagawa, H., Weber, H., Sagerer-Gerhardt, M., Weber, D. Sharma, T., Pitha, J. V., Lazzara, R., & Jackman, W. M. (2011). Open irrigated laser catheter produces deep lesions without thrombus formation. *Heart Rhythm, 8*(5), 32nd Annual Scientific Sessions: 262, PO1-83. https://www.researchgate.net/publication/274598472_Open-irrigated_laser_catheter_produces_deep_lesions_without_thrombus_or_steam_pop
9. Weber, H., Heinze, A., Ruprecht, L., & Sagerer-Gerhardt, M. (2018). Laser catheter modulation of the sinus node in the cure of inappropriate sinus tachycardia: Experimental and clinical results. *J Innovations CRM, 9*(7), 3232-3238. DOI: https://doi.org/10.19102/icrm.2018.090704
10. Weber, H., & Sagerer-Gerhard, M. (2014). Open-irrigated laser catheter ablation: relationship between the level of energy, myocardial thickness, and collateral damages in a dog model. *Europace, 16*(1), 142-48. DOI: https://doi.org/10.1093/europace/eut150
11. Weber, H., Schaur, P., & Sagerer-Gerhardt, M. (2019). Use of Light Sensor and Focused Local Atrial Electrogram Recordings for the Monitoring of Thermal Injury to the Esophagus and Lungs During Laser Catheter Ablation of the Posterior Atrial Walls: Preclinical In Vitro Porcine and In Vivo Canine Experimental Studies. *J Innovations CRM, 10*(7), 3723–31. DOI: https://doi.org/10.19102/icrm.2019.100703
12. Sagerer-Gerhardt, M., & Weber, H. (2016). Influence of catheter orientation on lesion formation in bovine myocardium by using an open-irrigated laser ablation catheter. *Lasers Med Sci, 31*(37), 1333-1338. DOI: https://doi.org/10.1007/s10103-016-1980-1
13. Whitaker, J., Rajani, R., Chubb, H., Gabrawi, M., Varela, M., Wright, M., Niederer, S., & D O'Neill, M. (2016). The role of myocardial wall thickness in atrial arrhythmogenesis. *Europace, 18*(12), 1758–1772. DOI: https://doi.org/10.1093/europace/euw014
14. Cunha, P. S., Laranjo, S., Monteiro, S., Almeida, I. G., Mendonça, T., Fontes, I., Ferreira R. C., Almeida, A. G., Didenko, M., & Oliveira, M. M. (2024). Left Atrial Wall Thickness Estimated by Cardiac CT: Implications for Catheter Ablation of Atrial Fibrillation. *J. Clin. Med, 13*(18), 5379. DOI: https://doi.org/10.3390/jcm13185379
15. Słodowska, K., Hołda, J., Dudkiewicz, D., Malinowska, K., Bolechała, F., Kopacz, P., Koziej, K., & Hołda, K. M. (2021). Thickness of the left atrial wall surrounding the left atrial appendage orifice. *J Cardiovasc Electrophysiol, 32*(8), 2262-2268. DOI: https://doi.org/10.1111/jce.15157
16. Nishimura, R. A., Seggewiss, H., & Schaff, H. V. (2017). Hypertrophic Obstructive Cardiomyopathy. Surgical Myectomy and Septal Ablation. *Circulation Research, 121*(7), 771-783. DOI: https://doi.org/10.1161/circresaha.116.309348
17. Obayashi, M., Kobayashi, S., Nanno, T., Hamada, Y., & Yano M. (2021). Relation between Oscillometric Measurement of Central Hemodynamics and Left Ventricular Hypertrophy in Hypertensive Patients. *Pulse, 9*(3-4), 116–124. DOI: https://doi.org/10.1159/000520006
18. Weber, H., Schmitz, L., Heinze, A., Ruprecht, L., & Sagerer-Gerhardt, M. (2017). The development of a laser catheter with improved mapping resolution and online monitoring of lesion formation during arrhythmia ablation. In C, Bellucci. (Ed.), Laser Ablation. Advances in Research and Applications (pp. 39-86). Nova Science Publishers, New York. Chapter 2. https://www.researchgate.net/publication/321681376_The_development_of_a_laser_catheter_with_improved_mapping_resolution_and_online_monitoring_of_lesion_formation_during_arrhythmia_ablation
19. Weber, H., Sagerer-Gerhardt, M., & Heinze, A. (2017). Laser catheter ablation of long-lasting persistent atrial fibrillation: Long term results. *J Atr Fibrillation, 10*(2), 1588. DOI: https://doi.org/10.4022/jafib.1588
20. Price, A., Leshen, Z., Hansen, J., Singh, I., Arora, P., Koblish, J., & Avitall, B. (2012). Novel Ablation Catheter Technology that Improves Mapping Resolution and Monitoring of Lesion Maturation. *The Journal of Innovations in Cardiac Rhythm Management, 3*(1), 599–609. DOI: https://doi.org/10.19102/icrm.2012.030102
21. Splinter, R. (2015). Laser catheter ablation of cardiac arrhythmias: Experimental and basic research and clinical results. In Topaz, O. (Ed.), Lasers in Cardiovascular Interventions (pp. 199-219). Springer, London. Chapter. DOI: https://doi.org/10.1007/978-1-4471-5220-0_16
22. Kushnir, A., Baraiya , C. R., Jankelson, L., Holmes, D., Aizer, A., Park, D., Bernstein, S., Spinelli, M. A., Garber, L., Yang, F., Rosinski, E., & Chinitz, L. A. (2025). Left atrial wall thickness correlates with pulmonary vein reconnection following atrial fibrillation ablation. *J Interv Card Electrophysiol, 68*(9), 1857-1863. DOI: https://doi.org/10.1007/s10840-025-02089-6
23. Vakhrushev, A. D., Condori, I., Korobchenko, L., Mitrofanova, L., Lebedev, D., & Mikhai¬lov, E. N. (2024). Laser catheter ablation of atrial zones with ganglionated plexi: impact on atrial fibrillation inducibility and the risk of esophageal damage in experimental settings. *Journal of Arrhythmology, 31*(2), 44-53. DOI: https://doi.org/10.35336/VA-1209

24. Francia, P., Viveros, D., Gigante, C., Falasconi, G., Penela, D., Soto-Iglesias, D., Landra, F., Teresi, L., Marti-Almor, J., Alderete, J., Saglietto, A., Bellido, A. F., Turturiello, D., Valeriano, C., Franco-Ocaña, P., Zaraket, F., Matiello, M., Fernández-Armenta, J., Antonio, R. S., … Berruezo, A. (2025). Differential and synergistic effects of right and left atrial ganglionated plexi ablation in patients undergoing Cardioneuroablation: results from the ELEGANCE multicenter study. *J Interventional Cardiac Electrophysiol, 68*(2), 195–202.
DOI: https://link.springer.com/journal/10840
25. Scherlag, B. J. (2015). Ablation of Ganglionated Plexi in the Long Term. Is Half a Loaf as Good as None? *Circ Arrhythm Electrophysiol, 8*(5), 1014-1016.
DOI: https://doi.org/10.1161/circep.115.003264
26. Del Monte, A., Della Rocca, D. G., Pannone, L., Vetta, G., Fernandez, M. C., Marcon, L., Doundoulakis, I., Mouram, S., Audiat, C., Zeriouh, S., Monaco, C., Al Housari, M., Betancur, A., Mené, R., Iacopino, S., Sorgente, A., Bala, G., Stroker, E., Sieira, J., … Chierchia, G. B. (2024). Pulsed field ablation of the right superior pulmonary vein prevents vagal responses via anterior right ganglionated plexus modulation. *Heart Rhythm, 21*(6), 780–787.
DOI: https://doi.org/10.1016/j.hrthm.2024.01.040
27. Creative commons. (n.d). Attribution-NonCommercial-NoDerivatives 4.0 International Legal Code.
http://creativecommons.org/licenses/by-nc-nd/4.0/
28. Pachon-M, J. C., Pachon-M, E. I., Pachon, C. T. C., Santillana-P, T. G., Lobo, T. J., Pachon-M, J. C,. Pachon, M. Z. C., & Clark, J. (2025). Impact of Vagal Effect on Atrial and Ventricular Refractoriness and Atrial Fibrillation: A Comparative Analysis Before and After Cardioneuroablation. *Heart Rhythm, S1547-5271*(25), 02951-0.
DOI: https://doi.org/10.1016/j.hrthm.2025.10.011
29. Pokushalov, E., Romanov, A., Katritsis, DA., Artyomenko, S., Shirokova, N., Karaskov, A., Mittal, S., & Steinberg, J. S. (2013). Ganglionated plexus ablation vs linear ablation in patients undergoing pulmonary vein isolation for persistent/long-standing persistent atrial fibrillation: A randomized comparison. *Heart Rhythm, 10*(9), 1280-6.
DOI: https://doi.org/10.1016/j.hrthm.2013.04.016
30. Splinter, R. (2025). Artificial intelligence in cardiac rhythm diagnostics and management: Challenges and opportunities. *Artif Intell Health, 2*(3), 107-124.
DOI: https://doi.org/10.36922/aih.8468